Communication

Cyclic 2,12-Porphyrinylene Nanorings As a Porphyrin Analogue of Cycloparaphenylenes

Hua-Wei Jiang, Takayuki Tanaka, Hirotaka Mori, Kyu Hyung Park, Dongho Kim, and Atsuhiro Osuka

J. Am. Chem. Soc., **Just Accepted Manuscript** • DOI: 10.1021/ja513102m • Publication Date (Web): 29 Jan 2015

Cyclic 2,12-Porphyrinylene Nanorings As a Porphyrin Analogue of Cycloparaphenylenes

Hua-Wei Jiang,† Takayuki Tanaka,† Hirotaka Mori,† Kyu Hyung Park,‡ Dongho Kim,*,‡ and Atsuhiro Osuka*,†

† Department of Chemistry, Graduate School of Science, Kyoto University, Sakyo-ku, Kyoto 606-8502, Japan

‡ Spectroscopy Laboratory for Functional π-Electronic Systems and Department of Chemistry, Yonsei University, Seoul 120-749, Korea

ABSTRACT: *β*-to-*β* Directly linked cyclic Ni(II) porphyrin trimer, tetramer, and pentamer (**[3]CP**, **[4]CP**, and **[5]CP**) have been synthesized by reaction of a 2,12-diborylated Ni(II) porphyrin with Pt(cod)Cl2 followed by reductive elimination. The structures of these cyclic porphyrin arrays have been revealed by X-ray diffraction analysis. The strain energies of these cyclic oligomers are calculated to be 77, 57, and 47 kcal/mol for **[3]CP**, **[4]CP**, and **[5]CP**, respectively. Intramolecular excitation energy hopping was observed between the $^3(d,d)$ states of the Ni(II) porphyrins with rates of 3.0, 4.4, and 4.6 ps for **[3]CP**, **[4]CP**, and **[5]CP**, respectively, reflecting the close proximity of the Ni(II) centers.

π-Conjugated nanorings have been attracting increasing attention in light of the curved conjugation along their peripheries, convex-concave host-guest interactions, synthetic challenges associated with achieving their highly distorted structures, and potential application in the bottom-up growth of uniform carbon nanotubes.[1,2] Recently, the invention of effective synthetic routes to cycloparaphenylenes ([n]CPPs), cyclic conjugated nanorings that consist of distorted benzene rings linked at the *para*-positions, has sparked a boom in this field (Chart 1).[3] Through the successful and independent explorations of [n]CPPs by Jasti, Itami, Yamago, and Isobe,[3-5] it has now been revealed that structural and electronic properties of [n]CPPs and related analogues depend on a delicate balance of strain and conjugation. The smallest CPP so far synthesized is [5]CPP that displays a considerably distorted structure.[6] Tetrameric macrocycles have been synthesized from larger polycyclic aromatic segments such as pyrene and chrysene.[7]

Cyclic porphyrin arrays have also been targets of extensive studies because of their potentials as models of artificial light-harvesting antenna complexes, hosts possessing convergent inward-pointing coordinating sites, and scaffolds to achieve efficient hole delocalization.[8] While non-covalently linked supramolecular cyclic porphyrins have been constructed in short steps with the aid of self-assembling strategies, covalently linked cyclic arrays are more difficult to construct,[9] mostly due to the entropic disadvantage in the final macrocyclization step. We described the successful synthetic realization of a *meso-meso* directly linked cyclic porphyrin tetramer, hexamer and octamer by Ag(I)-promoted oxidative coupling of 5,10-diaryl Zn(II) porphyrin unit.[10] However, these porphyrin rings are hardly regarded as porphyrin analogs of [n]CPPs because of their orthogonal linking topologies, which lead to disruption of the overall macrocyclic conjugation.

Chart 1. Structures of [n]CPPs, [4]cyclo-3,9-chrysenylene, and [n]CPs.

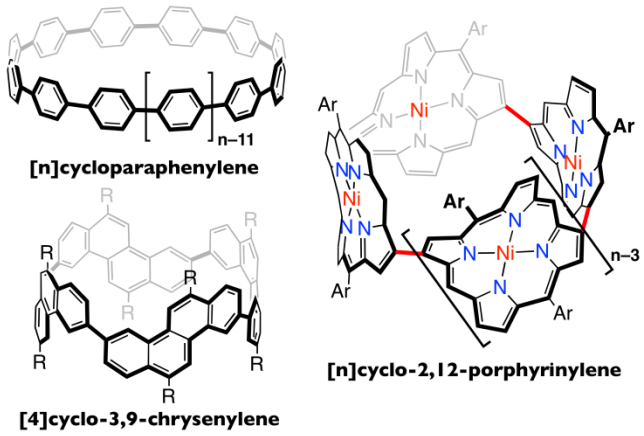

Scheme 1. Synthesis of *β*-borylated porphyrins.

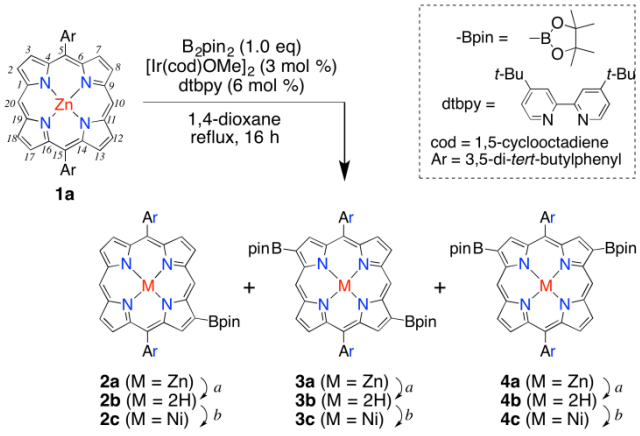

[a]conc. HCl, CH_2Cl_2, rt, 4 h. [b]$Ni(acac)_2$, toluene, reflux, overnight. acac = acetylacetonate. Ar = 3,5-di-*tert*-butylphenyl.

Here we report the synthesis and characterizations of cycloporphyrinylene nanorings, namely **[n]CPs** that consist of Ni(II) porphyrins directly linked at the 2- and 12-positions. As a macrocyclization strategy, we utilized a Pt(II)-mediated homo-coupling strategy developed by Yamago and Isobe.[4c,d] Along this strategy, we employed 2,12-diborylated Ni(II) porphyrin **3c** as a building block, in which the two connection points (2 and 12-positions, Scheme 1) are situated at the sterically least hindered locations with a diagonal separation distance of ca. 8.5 Å. In addition, Ni(II) porphyrins can adopt a ruffled or saddled conformation, which is favorable to reduce the overall ring strain of the resulting **[n]CPs**.

Ir-catalyzed borylations of porphyrins via C–H bond activation proceed regioselectively at the *β*-positions next to an unsubstituted *meso*-position, hence providing a reliable means for the preparation of *β*-borylated porphyrins.[11] 2,12-Diborylated Ni(II) porphyrin **3c**, a key precursor of **[n]CPs** in the present study, was formed in the borylation of **1c** but was very difficult to separate from an accompanying side product, 2,8-diborylated Ni(II) porphyrin **4c**, due to almost identical retention times on silica gel. Thus, **3c** was prepared via an indirect route. Borylation of 5,15-bis(3,5-di-*tert*-butylphenyl) porphyrin Zn(II) complex **1a** with equimolar bis(pinacolato)diboron under Ir(I)-catalyzed conditions gave a product mixture that contained *β*-borylated porphyrin products (Scheme 1). Separation by silica gel column chromatography and recycling preparative gel permeation chromatography (GPC) gave a mixture of **3a** and **4a** in 50% yield along with *β*-monoborylated porphyrin **2a** (26%). Fortunately, it was found that slow vapor diffusion of methanol into a solution of the product mixture in chloroform caused preferential recrystallization of **3a**. Almost complete separation of **3a** was possible via repeated recrystallization on large scale. Then, Zn(II) porphyrin **3a** was converted to Ni(II) porphyrin **3c** via acid-catalyzed de-zincation followed by Ni(II) insertion using $Ni(acac)_2$.

By following the one-pot reaction procedure of CPP macrocyclization,[4d] 2,12-diborylated Ni(II) porphyrin **3c** was reacted with equimolar $Pt(cod)Cl_2$ for 4 days at room temperature in the presence of cesium fluoride in THF. The resulting reaction mixture containing platinum-bridged porphyrins was refluxed in the presence of PPh_3 in toluene to induce reductive elimination (Scheme 2). After repeated separations, cyclic oligomers **[3]CP**, **[4]CP** and **[5]CP** were obtained in 5.0, 4.4 and 2.4% yields, respectively, in a reproducible manner. We attempted to optimize the reaction conditions by adjusting variables such as concentration, temperature, and adding extra equivalents of 1,5-cyclooctdiene, but we found that the conditions mentioned above have provided the best result with regard to the yields of **[n]CPs** with suppression of undesirable linear polymeric side products. The parent ion peaks for the **[n]CPs** were observed at *m/z* = 2220.90 (calcd. for $C_{144}H_{150}N_{12}Ni_3$ = 2221.02, $[M]^+$) for **[3]CP**, at *m/z* = 2961.48 (calcd. for $C_{192}H_{200}N_{16}Ni_4$ = 2961.36, $[M]^+$) for **[4]CP**, and at *m/z* = 3701.59 (calcd. for $C_{240}H_{250}N_{20}Ni_5$ = 3701.69, $[M]^+$) for **[5]CP** by MALDI-TOF MS. Although it was possible to detect cyclic oligomers with n values greater than **[5]CP** by MALDI-TOF MS, very poor yields made it extremely difficult to isolate them and so we abandoned full characterization of these products. It is worth to note that none of **[n]CPs** were formed from either the zinc or freebase forms of 2,12-diborylated porphyrin **3a** or **3b** under similar conditions, suggesting that a Ni(II) porphyrin scaffold is of vital importance in the successful formation of **[n]CPs**.

Scheme 2. Synthesis of 2,12-porphyrinylene nanorings.

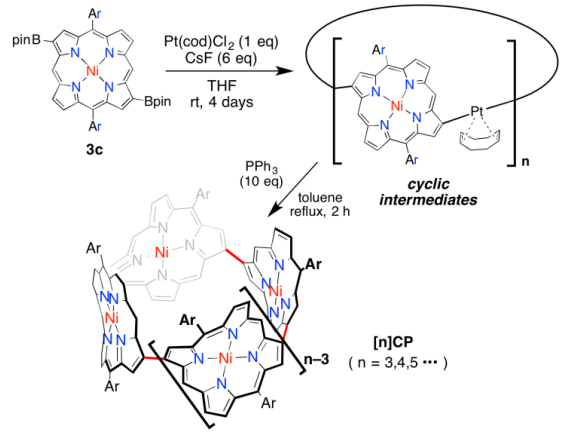

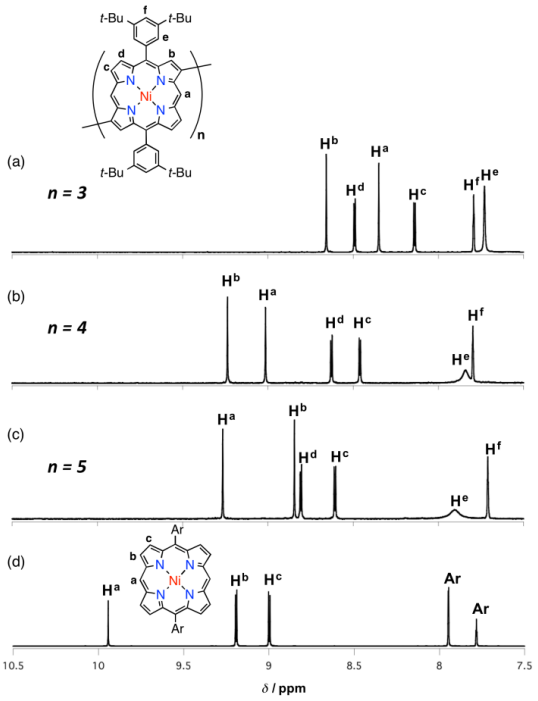

Figure 1. ^{1}H NMR spectra of (a) **[3]CP**, (b) **[4]CP**, (c) **[5]CP** and (d) **1c** in the aromatic region in $CDCl_3$ at room temperature.

All the ^{1}H NMR spectra of **[3]CP**, **[4]CP**, and **[5]CP** feature a distinct signature set of signals consisting of one singlet associated with the *meso*-protons (H^a), one singlet (H^b) and two doublets (H^c and H^d) corresponding to the *β*-protons, indicating their highly symmetric structures (Figure 1). The assignments of the signals have been fully performed through 2D NOESY experiments. The protons at the porphyrin peripheries were shifted up field compared with the corresponding peaks of the monomer **1c**, reflecting the influence of the ring-currents of adjacent porphyrins.[12] Such trend becomes more prominent in the order of **[5]CP** < **[4]CP** < **3[CP]**.

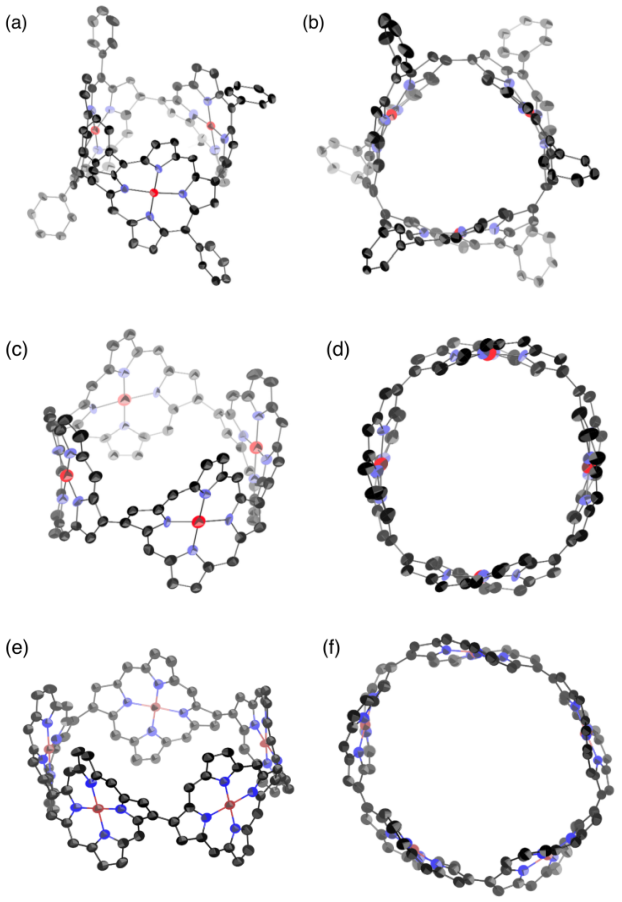

Figure 2. X-ray crystal structures of **[3]CP** (a and b), **[4]CP** (c and d), and **[5]CP** (e and f). *tert*-Butyl groups in (a) and (b), *meso*-Aryl groups in (c), (d), (e) and (f), solvent molecules, and hydrogen atoms are omitted for clarity. The ellipsoids are scaled to the 30% probability. Disorders were found for **[5]CP**.

To our delight, crystals of **[3]CP**, **[4]CP** and **[5]CP** suitable for single-crystal X-ray diffraction analysis were obtained by slow solvent diffusion of a methanol/heptane mixture into their respective solutions in chloroform. Definitive structural determinations were then accomplished by revealing [n]CPP-like hoop structures (Figure 2). In all cases, Ni(II) porphyrins take severely saddled conformations, which is likely important to accommodate large distortion arising from the hoop-like cyclic architectures. The averaged C_β—C_β bond lengths and diameters of the nanorings are 1.47 and 9.32 Å, and 1.45 and 11.95 Å, and 1.48 and 15.60 Å for **[3]CP**, **[4]CP**, and **[5]CP**, respectively. Upon increasing the ring size, the Ni(II)—Ni(II) center-to-center sepration distances are increased to be 7.36, 8.31, and 8.80 Å for **[3]CP**, **[4]CP**, and **[5]CP**, respectively. These structural features are comparable to those of DFT optimized structures (See SI).

The UV/Vis absorption spectra of **[3]CP**, **[4]CP**, and **[5]CP** exhibit broader Soret-bands and red-shifted Q-like bands as compared with those of monomer **3c** (Figure 3); Soret-like bands are observed at 409, 414, and 423 nm, and Q-like bands are observed at 552 and 593 nm, 548 and 595 nm, and 535 and 595 nm, for **[3]CP**, **[4]CP**, and **[5]CP**, respectively. Curiously, the peak positions in the absorption spectra of **[3]CP**, **[4]CP**, and **[5]CP** are not so much changed, implying similar exciton coupling interactions. These spectral features are reminiscent of those of cyclic Zn(II) porphyrin rings directly linked at the 5,10-positions,[10] in line with the cyclic structures.

The electrochemical properties of **1c**, **[3]CP**, **[4]CP**, and **[5]CP** were investigated by cyclic voltammetry and differential pulse voltammetry (SI). The monomer **1c** shows two oxidation potentials at 0.50 and 1.00 V and a reduction potential at –1.78 V versus ferrocene/ferronenium ion couple, which leads to an electrochemical HOMO–LUMO gap of 2.28 eV. **[3]CP** exhibits split oxidation potentials at 0.36 and 0.60 V and split reduction potentials at –1.71 and –1.91 V, reflecting the electronic interactions among the Ni(II) porphyrins in the ring. Similar but more complicated split potentials were observed at 0.41, 0.58 and 0.64 V, and –1.64, –1.86, and –2.05 V for **[4]CP**, and 0.46, and 0.64 V, and –1.58, –1.65, and –1.80 V for **[5]CP**. Upon increase in the ring size, these potentials are shifted to the anodic side.

The excited state dynamics of **[n]CPs** exhibited ultrafast decay dynamics that are characteristic of Ni(II) porphyrin derivatives (SI).[13] All **[n]CPs** exhibited broad excited-state absorption bands (ESA) from 700 to 850 nm, which showed very rapid decays. Simultaneous peak shifts in the ground-state bleaching (GSB) around 600 nm and ESA near 500 nm noticeably altered the shape of the initial transient absorption spectra. This initial decay with τ = 0.6 ps, common to all **[n]CPs**, is associated with the transition from the lowest energy $^1(\pi,\pi^*)$ state to Ni(II)-centered $^3(d,d)$ state and is responsible for the TA spectral changes on sub-picosecond timescale. Relaxed $^3(d,d)$ state decayed to the ground state with time constants of 50, 40, and 30 ps for **[3]CP**, **[4]CP**, and **[5]CP**, respectively (SI). Decreasing lifetimes of $^3(d,d)$ state can be rationalized in terms of increasing nonradiative decay rate with increasing molecular size.

Interestingly, the transient absorption anisotropy for **[3]CP**, **[4]CP**, and **[5]CP** decayed from the respective initial anisotropy values of r_o = 0.05, 0.019, and 0.047 with time constants of 1.0, 1.1, and 1.3 ps, respectively (SI). In contrast to the high initial anisotropy value of **1c** (r_o = 0.14), the observed initial low anisotropy values of **CP** are caused as a consequence of efficient excitation energy hopping along the porphyrin nanorings. While the anisotropy decay of **1c** showed a simple rotational diffusion with a time constant of 370 ps, depolarization processes of **CP** contained ultrafast interchromophoric excitonic process. Considering sub-picosecond lifetimes of the $^1(\pi,\pi^*)$ state of the Ni(II) porphyrins, anisotropy decays of **CP** can be interpreted in terms of EET between the metal-centered $^3(d,d)$ states. Based on a polygon model, the excitation energy hopping times have been evaluated to be 3.0, 4.4, and 4.6 ps for **[3]CP**, **[4]CP**, and **[5]CP**, respectively. Due to metal-localized orbital distribution of $^3(d,d)$ states, the EET processes in **[n]CPs** are less efficient than those in $^1(\pi,\pi^*)$ states of *meso-meso* directly linked Zn(II) porphyrin rings that occur with time constants of 0.12, 0.34, and 0.24 ps for tetramer, hexamer, and octamer, respectively.[10] The small increase in energy hopping time with increasing ring size is presumably attributed to increasing Ni(II)—Ni(II) center-to-center separation distances between the neighboring porphyrin chromophores.

MO calculations on these **[n]CPs** were performed using the Gaussian 09 package at the B3LYP/6-31G*(for C, H, N) +LANL2DZ (for Ni) level. While the HOMOs and LUMOs of **[3]CP** and **[5]CP** are both degenerate, being similar to those of monomeric porphyrins, the HOMO and LUMO of **[4]CP** are both non-degenerate as a consequence of effective bond-

ing interactions in the LUMO and anti-bonding interaction in HOMO–1, a phenomena observed only for even-membered nanorings as a characteristic feature of direct *β*-*β* connectivity. This odd/even feature can also be seen in the calculated MOs of **[6]CP** (SI). Finally, the ring strain energies (*ΔH*) have been calculated according to the homodesmotic reaction model[14] to be 77.4, 57.7, and 47.4 kcal/mol for **[3]CP**, **[4]CP**, and **[5]CP**, respectively. Therefore, it is possible to infer that **[3]CP**, **[4]CP**, and **[5]CP**, are highly strained nanorings comparable to [n]CPPs.[15]

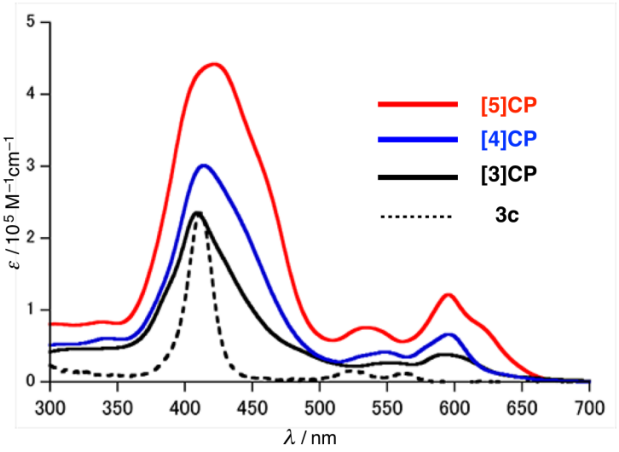

Figure 3. UV/Vis absorption spectra of **[3]CP**, **[4]CP** and **[5]CP** in CH_2Cl_2.

In summary, cyclo-2,12-porphyrinylene nanorings **[3]CP**, **[4]CP**, and **[5]CP** have been synthesized as the first porphyrin analogues of CPPs via Pt-mediated cyclization of a 2,12-diborylated Ni(II) porphyrin followed by reductive elimination. Among these nanorings, **[3]CP** is the most strained system with a calculated strain energy of 77.4 kcal/mol. The conjugative interactions have been calculated to be effective only for even-membered **[n]CPs**, which results in non-degenerate HOMO and LUMO orbitals for **[4]CP**, while such conjugative interactions are ineffective for **[3]CP** and **[5]CP**. Exploration of further elaborate architectures utilizing alternative metal complexes and detailed photophysical analysis of efficient energy transfer along these architectures is an active area of research in our laboratory.

ASSOCIATED CONTENT

Supporting Information. Experimental procedure, complete characterizations (NMR, UV/vis, MS, CV), DFT calculations, excited-state dynamics, and X-ray crystallographic data for **3a-c**, **[3]CP**, **[4]CP**, and **[5]CP**. This material is available free of charge via the Internet at http://pubs.acs.org.

AUTHOR INFORMATION

Corresponding Author

E-mail: osuka@kuchem.kyoto-u.ac.jp
E-mail: dongho@yonsei.ac.kr

Notes

The authors declare no competing financial interest.

ACKNOWLEDGMENT

This work was supported by Grant-in-Aid from JSPS (No. 25220802 (Scientific Research (S) and No. 26810021 (Young Scientist (B)). The work at Yonsei was supported by the Global Research Laboratory (GRL) Program funded by the Ministry of Science, ICT & Future, Korea (2013K1A1A2A02050183). The authors thank Prof. Hiromitsu Maeda and Dr. Yuya Bando (Ritsumeikan University) for MALDI-TOF MS measurement.

REFERENCES

(1) (a) Girreser, U.; Giuffrida, D.; Kohnke, F. H.; Mathias, J. P.; Philp, D.; Stoddart, J. F. *Pure Appl. Chem.* **1993**, *65*, 119. (b) Scott, L. T. *Angew. Chem. Int. Ed.* **2003**, *42*, 4133. (c) Tahara, K.; Tobe, Y. *Chem. Rev.* **2006**, *106*, 5274. (d) Kawase, T.; Kurata, H. *Chem. Rev.* **2006**, *106*, 5250. (e) Eisenberg, D.; Shenhar, R.; Rabinovitz, M. *Chem. Soc. Rev.* **2010**, *39*, 2879. (f) Iyoda, M.; Yamakawa, J.; Rahman, M. J. *Angew. Chem. Int. Ed.* **2011**, *50*, 10522.

(2) (a) Jasti, R.; Bertozzi, C. R. *Chem. Phys. Lett*. **2010**, *494*, 1. (b) Omachi, H.; Nakayama, T.; Takahashi, E.; Segawa, Y.; Itami, K. *Nat. Chem*. **2013**, *5*, 572.

(3) Recent reviews: (a) Omachi, H.; Segawa, Y.; Itami, K. *Acc. Chem. Res.* **2012**, *45*, 1378. (b) Hirst, E. S.; Jasti, R. *J. Org. Chem.* **2012**, *77*, 10473. (c) Sisto, T. J.; Jasti, R. *Synlett* **2012**, *23*, 483. (d) Yamago, S.; Kayahara, E.; Iwamoto, T. *Chem. Rec.* **2014**, *14*, 84.

(4) (a) Jasti, R.; Bhattacharjee, J.; Neaton, J. B.; Bertozzi, C. R. *J. Am. Chem. Soc.* **2008**, *130*, 17646. (b) Takaba, H.; Omachi, H.; Yamamoto, Y.; Bouffard, J.; Itami, K. *Angew. Chem. Int. Ed.* **2009**, *48*, 6112. (c) Yamago, S.; Watanabe, Y.; Iwamoto, T. *Angew. Chem. Int. Ed.* **2010**, *49*, 757. (d) Hitosugi, S.; Nakanishi, W.; Yamasaki, T.; Isobe, H. *Nat. Commun*. **2011**, *2*, 492.

(5) (a) Iwamoto, T.; Watanabe, Y.; Sakamoto, Y.; Suzuki, T.; Yamago, S. *J. Am. Chem. Soc.* **2011**, *133*, 8354. (b) Xia, J.; Jasti, R. *Angew. Chem. Int. Ed*. **2012**, *51*, 2474. (c) Yagi, A.; Segawa, Y.; Itami, K. *J. Am. Chem. Soc.* **2012**, *134*, 2962.

(6) (a) Kayahara, E.; Patel, V. K.; Yamago, S. *J. Am. Chem. Soc*. **2014**, *136*, 2284. (b) Evans, P. J.; Darzi, E. R.; Jasti, R. *Nat. Chem.* **2014**, *6*, 404.

(7) (a) Yagi, A.; Venkataramana, G.; Segawa, Y.; Itami, K. *Chem. Commun.* **2014**, *50*, 957. (b) Iwamoto, T.; Kayahara, E.; Yasuda, N.; Suzuki, T.; Yamago, S. *Angew. Chem. Int. Ed.* **2014**, *53*, 6430. (c) Hitosugi, S.; Yamasaki, T.; Isobe, H. *J. Am. Chem. Soc.* **2012**, *134*, 12442. (d) Matsuno, T.; Kamata, S.; Hitosugi, S.; Isobe, H. *Chem. Sci.* **2013**, *4*, 3179.

(8) Cyclic porphyrin arrays: (a) Anderson, S.; Anderson, H. L.; Sanders, J. K. M. *Acc. Chem. Res.* **1993**, *26*, 469. (b) Satake, A.; Kobuke, Y. *Tetrahedron* **2005**, *61*, 13. (c) Nakamura, Y.; Aratani, N.; Osuka, A. *Chem. Soc. Rev.* **2007**, *36*, 831. (d) Aratani, N.; Kim, D.; Osuka, A. *Acc. Chem. Res.* **2009**, *42*, 1922. (e) Kato, A.; Sugiura, K.; Miyasaka, H.; Tanaka, H.; Kawai, T.; Sugimoto, M.; Yamashita, M. *Chem. Lett.* **2004**, 33, 578. (f) Aratani, N.; Osuka, A. *Chem. Commun*. **2008**, 4076. (g) Jiang, H. -W.; Ham, S.; Aratani, N.; Kim, D.; Osuka, A. *Chem. -Eur. J.* **2013**, *19*, 13328. (h) Parkinson, P.; Knappke, C. E. I.; Kamonsutthipaijit, N.; Sirithip, K.; Matichak, J. D.; Anderson, H. L.; Herz, L. M. *J. Am. Chem. Soc*. **2014**, *136*, 8217.

(9) Template synthesis of cyclic porphyrin arrays: (a) Anderson, H. L.; Sanders, J. K. M. *Angew. Chem. Int. Ed. Engl.* **1990**, *29*, 1400. (b) Yu, L.; Lindsey, J. *J. Org. Chem.* **2001**, *66*, 7402. (c) Rucareanu, S.; Schuwey, A. Gossauer, A. *J. Am. Chem. Soc.* **2006**, *128*, 3396. (d) O'Sullivan, M. C.; Sprafke, J. K.; Kondratuk, D. V.; Rinfray, C.; Claridge, T. D. W.; Saywell, A.; Blunt, M.; O'Shea, J. N.; Beton, P. H.; Malfois, M.; Anderson, H. L. *Nature* **2011**, *469*, 72.

(10) Nakamura, Y.; Hwang, I. -W.; Aratani, N.; Ahn, T. K.; Ko, D. M.; Takagi, A.; Kawai, T.; Matsumoto, T.; Kim, D.; Osuka, A. *J. Am. Chem. Soc*. **2005**, *127*, 236.

(11) (a) Hata, H.; Shinokubo, H.; Osuka, A. *J. Am. Chem. Soc*. **2005**, *127*, 8264. (b) Shinokubo, H.; Osuka, A. *Chem. Commun*. **2009**, 1011. (c) Yorimitsu, H.; Osuka, A. *Asian J. Org. Chem.* **2013**, *2*, 356.

(12) The chemical shifts of H^b are 8.66, 9.25, and 8.85 for **[3]CP**, **[4]CP**, and **5[CP]**, respectively. These have been interpreted in terms

of different ring current effects of the neighboring porphyrin. The averaged C—C bond distances of the direct connection are 1.47, 1.45, and 1.48 Å.

(13) Zhang, X.; Wasinger, E. C.; Muresan, A. Z.; Attenkofer, K.; Jennings, G.; Lindsey, J. S.; Chen, L. X. *J. Phys. Chem. A* **2007**, *111*, 11736.

(14) (a) Segawa, Y.; Omachi, H.; Itami, K. *Org. Lett*. **2010**, *12*, 2262. (b) Bachrach, S. M.; Stück, D. *J. Org. Chem*. **2010**, *75*, 6595. (c) George, P.; Trachtman, M.; Bock, C. W.; Brett, A. M. *Tetrahedron* **1976**, *32*, 317.

(15) Strain associated with wheel formation is considered to be accommodated within flexible Ni(II) porphyrin skeletons.

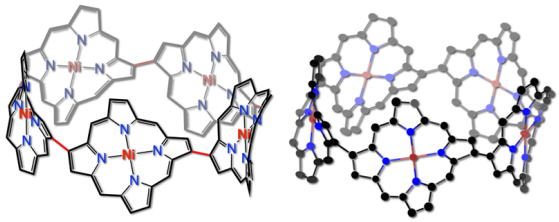

2,12-Linked Porphyrin Nanorings